

Addendum to: Edge-Unfolding Nearly Flat Convex Caps

Joseph O'Rourke*

September 2, 2017

Abstract

This addendum to [O'R17] establishes that a nearly flat acutely triangulated convex cap in the sense of that paper can be edge-unfolded even if closed to a polyhedron by adding the convex polygonal base under the cap.

1 Introduction

The paper [O'R17] established that every sufficiently flat acutely triangulated convex cap has an edge-unfolding to a non-overlapping simple polygon, i.e., a *net*. I used the term “convex cap” in the following sense (where $\phi(f)$ is the angle the normal to face f makes with the z -axis):

Define a *convex cap* \mathcal{C} of angle Φ to be $C = \mathcal{P} \cap H$ for some \mathcal{P} and H , such that $\phi(f) \leq \Phi$ for all f in \mathcal{C} . [...] Note that \mathcal{C} is not a closed polyhedron; it has no “bottom,” but rather a boundary $\partial\mathcal{C}$.

This note proves that same claim holds even when \mathcal{C} is closed to a polyhedron by adjoining the convex base face B bounded by $\partial\mathcal{C}$. Eventually this addendum will be incorporated into a future version [O'R17]. For now we assume familiarity with that paper, and especially the section below, the most relevant portions of which we reproduce verbatim. Ellisions are marked by “[...]”

2 Angle-Monotone Spanning Forest

[...]

*Department of Computer Science, Smith College, Northampton, MA, USA. jorourke@smith.edu.

2.1 Angle-Monotone Spanning Forest

“It was proved in [LO17] that every nonobtuse triangulation G of a convex region C has a boundary-rooted spanning forest F of C , with all paths in F 90° -monotone. We describe the proof and simple construction algorithm before detailing the changes necessary for acute triangulations.

Some internal vertex q of G is selected, and the plane partitioned into four 90° -quadrants Q_0, Q_1, Q_2, Q_3 by orthogonal lines through v . Each quadrant is closed along one axis and open on its counterclockwise axis; q is considered in Q_0 and not in the others, so the quadrants partition the plane. It will simplify matters later if we orient the axes so that no vertex except for q lies on the axes, which is clearly always possible. Then paths are grown within each quadrant independently, as follows. A path is grown from any vertex $v \in Q_i$ not yet included in the forest F_i , stopping when it reaches either a vertex already in F_i , or ∂C . These paths never leave Q_i , and result in a forest F_i spanning the vertices in Q_i . No cycle can occur because a path is grown from v only when v is not already in F_i ; so v becomes a leaf of a tree in F_i . Then $F = F_1 \cup F_2 \cup F_3 \cup F_4$.

We cannot follow this construction exactly in our situation of an acute triangulation G , because the “quadrants” for θ -monotone paths for $\theta = 90^\circ - \Delta\theta < 90^\circ$ cannot cover the plane exactly: They leave a thin $4\Delta\theta$ angular gap; call the cone of this aperture g . We proceed as follows. Identify an internal vertex q of G so that it is possible to orient the cone-gap g , apexed at q , so that g contains no internal vertices of G . See Fig. 1 for an example. Then we proceed just as in [LO17]: paths are grown within each Q_i , forming four forests F_i , each composed of θ -monotone paths.

It remains to argue that there always is such a q at which to apex cone-gap g . Although it is natural to imagine q as centrally located (as in Fig. 1), it is possible that G is so dense with vertices that such a central location is not possible. However, it is clear that the vertex q that is closest to ∂C will suffice: aim g along the shortest path from q to ∂C . Then g might include several vertices on ∂C , but it cannot contain any internal vertices of G , as they would be closer to ∂C . Again we could rotate the axes slightly so that no vertex except for q lies on an axis.”

[...] (End quoted text.)

3 Unfolding the Base B

By our definition of a convex cap, its boundary ∂C lies in a plane, and so bounds a convex polygonal base B . We assume that, unlike the cap C , B is not triangulated, and so must be unfolded as an intact unit. (Of course, it can be unfolded as a unit even if triangulated.)

Let C_\perp be the unfolded net of C produced by the algorithm in [O’R17]. If some edge e of C_\perp lies on the convex hull of C_\perp , then B can be “flipped out” to B' around e by cutting all edges of ∂C except for e . Because B' is convex and is attached to the hull of C_\perp , it is clear there is no overlap, and we

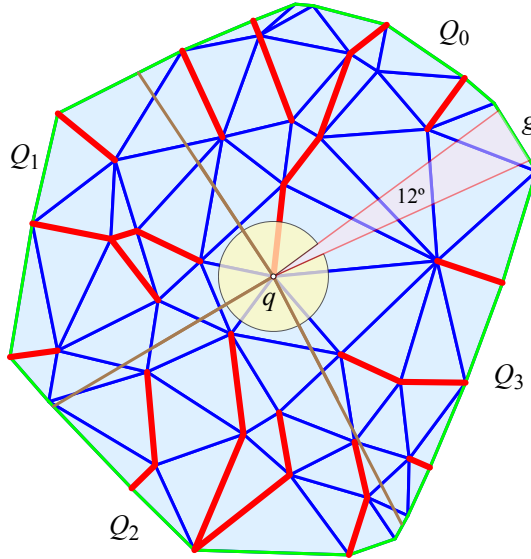


Figure 1: Here the near-quadrants Q_i have width $\theta = 87^\circ$, so the gap g has angle $4\Delta\theta = 12^\circ$.

would be finished. In fact this is the proof path we will follow, but it is not as straightforward as it might seem.

3.1 Obstructions

We now argue that there is an arbitrarily flat convex cap \mathcal{C} and a spanning cut forest \mathcal{F} such that there is no such edge e of C_\perp to which to attach B' without overlap. First, we look at a “real” unfolding to see what form the obstruction might take. Fig. 2 shows a portion of C_\perp , identifying a particular edge e which is tilted inside the hull and would lead to overlap were B' attached there. However, even in this example, there are many other candidates for e that would suffice as B' 's attachment. This suggests the next question: Is there a cap \mathcal{C} and a cut forest \mathcal{F} such that every edge of C_\perp is similarly titled inside the hull, leaving no “safe” attachment edge for B' ? The answer is YES. We only sketch the argument before discussing in more detail how to circumvent this counterexample.

Let \mathcal{C} be a cap whose boundary $\partial\mathcal{C}$ is a 12-sided regular polygon (i.e., a dodecagon). For the construction to work, we need at least a 9-sided polygon; 12 makes it visually clearer. The cut forest \mathcal{F} is as illustrated in Fig. 3: one tree in \mathcal{F} is a 2-path from the center of \mathcal{C} , and all the others trees are single segments. The key property is that each segment creates a very shallow angle with $\partial\mathcal{C}$.

We arrange near-zero curvature at the central vertex, and all the other vertices have the same curvature $\omega > 0$. Because of the shallow angle they form

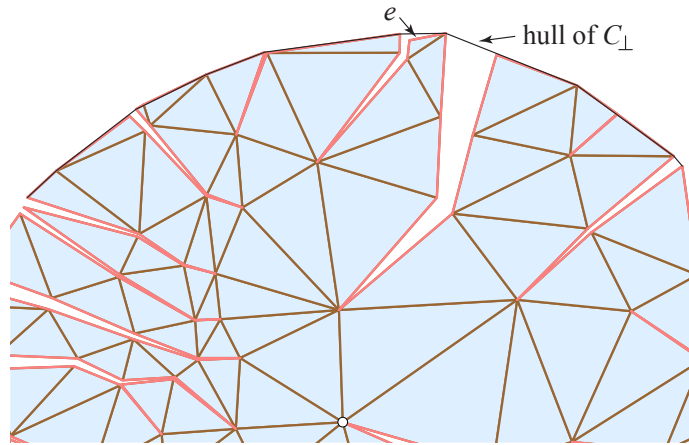


Figure 2: Detail from Fig. 24 of [O'R17], with a portion of the convex hull marked.

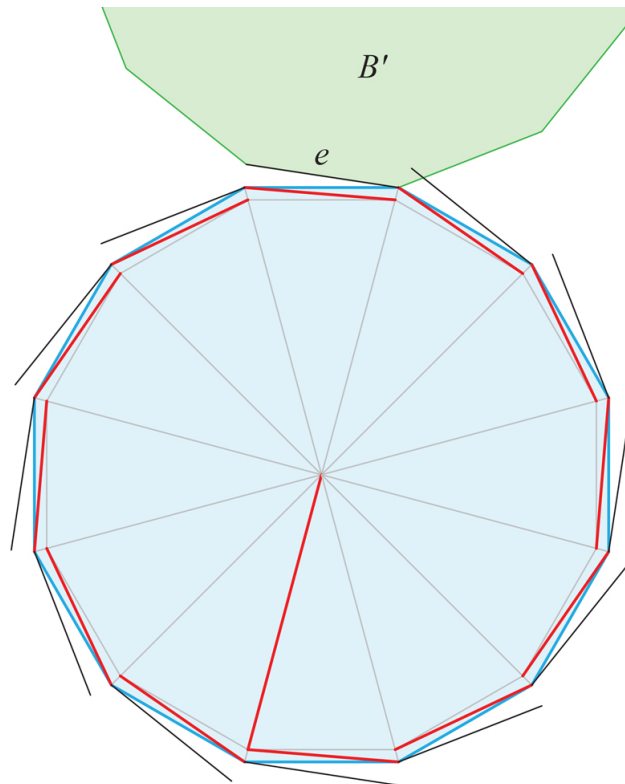


Figure 3: No edge of C_{\perp} is a convex hull edge. The cut forest F is shown red, $\partial\mathcal{C}$ is blue, developed edges of C_{\perp} black.

with $\partial\mathcal{C}$, the opening gap caused by cutting each segment is nearly orthogonal to the cut segment. With the internal angle of a 12-gon $\frac{5}{6}\pi$, the exterior angle between B and a reflected copy B' of B is $\frac{2}{6}\pi = 60^\circ < 90^\circ$. This allows the orthogonally jutting rotation of each boundary edge to penetrate into a reflected B' , reflected about the next edge e counterclockwise, as illustrated.

There is no impediment to realizing this example in 3D so that the curvatures ω suffice to render every boundary edge of C_\perp leading to overlap with B' . Moreover, this could be accomplished for an arbitrarily flat \mathcal{C} by increasing the number of sides of the n -gon base so that even a very small ω results in overlap. These claims will not be justified further, as they only serve to motivate the next steps.

3.2 Quadrant-based forest F

The reason the preceding counterexample does not present an insurmountable obstacle is that the spanning forest F selected in the planar projection graph G of \mathcal{C} is not arbitrary, but instead is based on the quadrants illustrated in Fig. 1. We now show that the quadrant-based forest F leads to an edge e of C_\perp to which to attach the reflected base B' .

A reminder on the notation we are employing: \mathcal{C} is the convex cap in \mathbb{R}^3 , C is its projection on the xy -plane, F the spanning forest in that plane, \mathcal{F} the lift of the forest, and C_\perp is the development of the cap \mathcal{C} after cutting \mathcal{F} .

Let $v \in \partial\mathcal{C}$ be a vertex on the boundary of the projection C that is a root of a tree in the forest F . Rather than viewing the lift, cut, and development as producing C_\perp , it will help to view the movement of v in the plane caused by opening the curvatures along the cut paths terminating at v . As we saw in Section 8 of [O'R17], we can view each cut path Q to v as two planar polygonal chains L and R which are initially identical, and then open at each vertex v_i along Q by the curvatures ω_i . Here we are only interested in the final planar displacement of the root v , the endpoint of the chain. Let v and v' be the original and displaced versions of v , i.e., the last vertices of L and R . The *gap segment* vv' represents the gap at the boundary of C_\perp caused by opening the cuts in F to v , visible, for example, in Fig. 2.

The gap segment vv' is caused by the composition of several (small) rotations about different centers, the vertices along Q . It is well-known that vv' is equivalent to a single rotation about a (generally) different center c , which we'll call the *composite center of rotation*. We claim that, for sufficiently small ω_i , c is either inside the convex hull of Q , or arbitrarily close to the boundary of the hull. This claim is justified in the Appendix by Lemma 2.

Returning to Fig. 3, the centers of rotation in F were arranged so that the gap segments were nearly orthogonal to $\partial\mathcal{C}$, so that they “juttied out” and caused overlap with the reflected B' . We now argue first, that a different arrangement of centers of rotation can produce “safe” gap segments, and second, that this can be achieved by a quadrant-based spanning forest F .

Arrange an edge $e = (v, u)$ of $\partial\mathcal{C}$ to be topmost and horizontal and crossing the vertical quadrant boundary, and suppose both v and u are roots of cut trees

in F . We call e a *locally safe edge* if the composite centers of rotation c_v and c_u for the trees incident to v and u fall underneath e , as illustrated in Fig. 4. For then the gap segments angle down below e , making e a safe candidate for the attachment of B' .

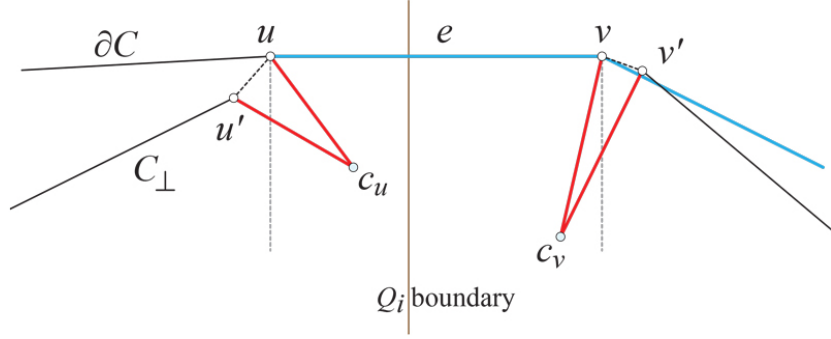


Figure 4: Safe edge e .

Returning to Fig. 1, we now argue that what was there called the gap edge g of ∂C can serve as a safe edge e . As in that figure, let q be the quadrants origin. The shortest path γ on \mathcal{C} to ∂C is orthogonal to a boundary edge e . The development of the geodesic γ is a straight line. Use this straight line as the vertical axis of the quadrants, with e horizontal. Now, because the spanning forest algorithm grows edges within the quadrant wedges, we are guaranteed that all edges of a tree incident to the endpoints of e are slanted such that they angle strictly vertically underneath e , as illustrated in Fig. 5. The strictness follows because the wedges are $\Delta\theta$ less than 90° .

Now applying Lemma 2, we obtain that the composite center of rotation is underneath e . Even though that lemma allows the true center to be slightly outside the hull of the rotation centers, that the wedges have angle less than 90° permits the conclusion that the true center is in the hull for sufficiently small ω_i , and therefore strictly underneath e . Thus we know that e is a locally safe edge.

But now it is easy to reapply this argument to conclude that none of the gap segments for other vertices around ∂C are angled above the horizontal, and so e is in fact globally safe. Thus we can attach the reflected base B' along e without overlap. This proves:

Theorem 1 *A convex polyhedron consisting of a nearly flat acutely triangulated convex cap \mathcal{C} joined along ∂C to a base B can be edge-unfolded without overlap, for sufficiently small cap curvature Ω .*

Using the error between the true and approximate composite rotation centers $\delta = \frac{1}{2} \sum_i \ell_i \omega_i$ from Lemma 1, and crudely summarizing this as $\delta = L\omega/2$ for a total chain length L , a calculation shows the wedge slant $\Delta\theta$ leads to “sufficiently

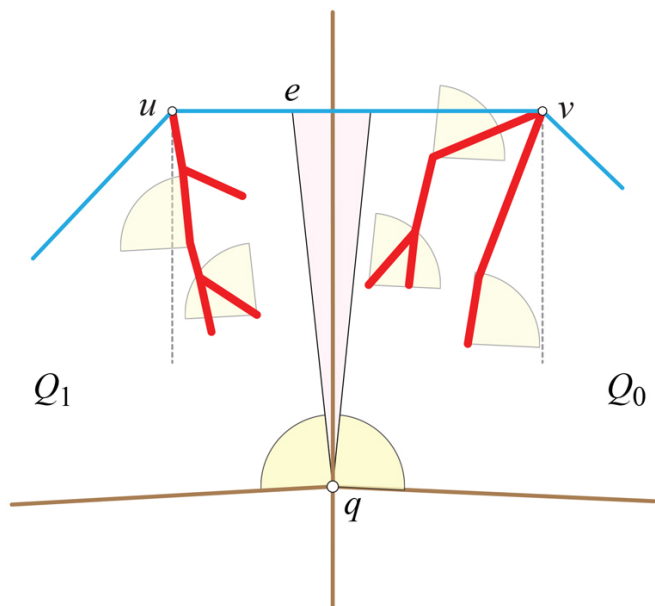


Figure 5: The trees incident to the endpoints of e have composite centers of rotation underneath e .

small” curvatures satisfied if $\omega \lesssim 2\Delta\theta$. But already we know that

$$\Omega < \pi\Phi^2 < \pi(0.3\sqrt{\Delta\theta})^2 \approx 0.28\Delta\theta,$$

and because $\omega < \Omega$ for any one tree of F , the curvatures are already “sufficiently small” from other constraints.

An illustration is shown in Fig. 6. The selection of e in this example does not follow the proof exactly just due to limitations of my implementation (q is not closest to $\partial\mathcal{C}$ and e is not orthogonal to the vertical quadrant axis), but it illustrates how e is locally and indeed globally safe. (In this and in most examples, there are many safe edges.)

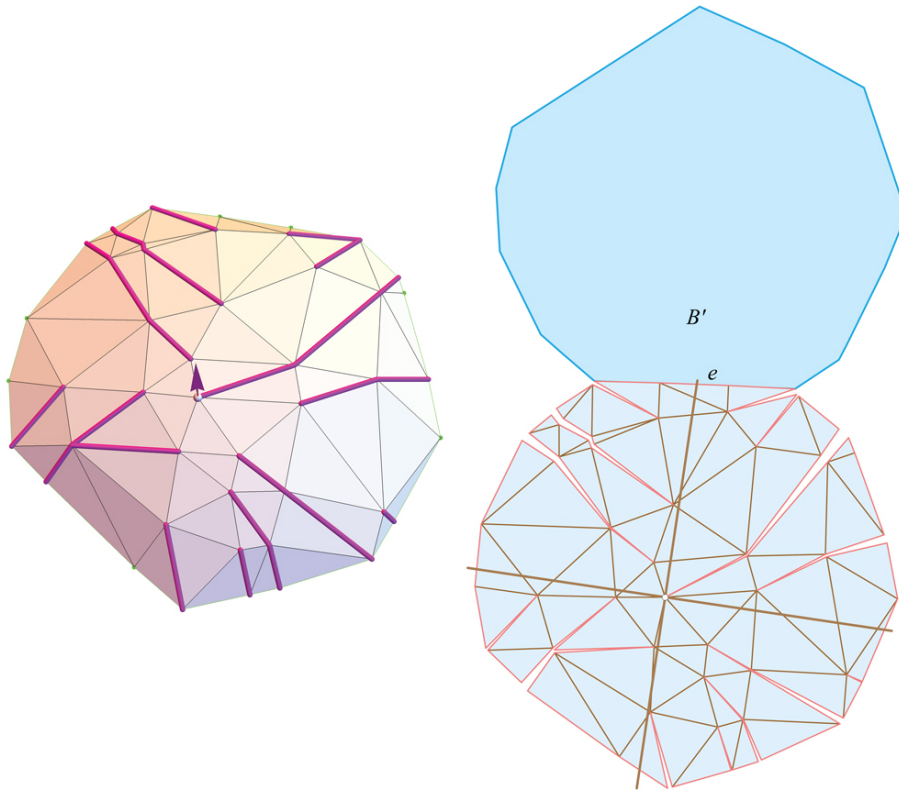


Figure 6: Cap \mathcal{C} (left) and an edge-unfolding (right), including base B flipped across safe edge e .

Appendix

We need a lemma that allows us to conclude that, for small curvatures, the effect of the rotations along a cut path Q to a boundary vertex $v \in \partial C$ is equivalent to one rotation from a point in the convex hull of the vertices along Q .

Lemma 1 *Let $R_i(\omega_i, p_i)$ be a two-dimensional rotation by angle $\omega_i \geq 0$ about point p_i , for $i = 1, \dots, k$. Then, for sufficiently small ω_i , the result of composing the k rotations R_i is equivalent to one rotation about a center-of-gravity rotation center: the sum of the p_i weighted by the angles:*

$$R_1(\varepsilon\omega_1, p_1) \circ \dots \circ R_k(\varepsilon\omega_k, p_k) \rightarrow R(\varepsilon\omega, p)$$

as $\varepsilon \rightarrow 0$, where

$$\omega = \sum_i \omega_i$$

and

$$p = (\omega_1 p_1 + \dots + \omega_k p_k) / \omega .$$

The role of ε is to ensure all the angles approach 0. Equivalently (and more appropriate in our context), we can just think of the ω_i as “sufficiently small.” This proposition is illustrated in Fig. 7 for a polygonal chain.

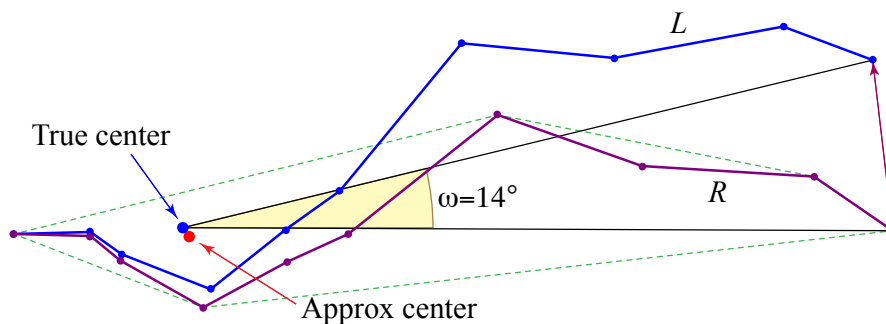


Figure 7: Comparison of true composite center of rotation, and the approximate center-of-gravity center. Here R is fixed and L obtained by ω_i rotations.

Proof: It is well-known that the composition of two rotations by angles ω_1, ω_2 about different centers p_1, p_2 is equivalent to one rotation by $\omega_1 + \omega_2$ about a (generally) different center c .¹ Consequently, the same holds for the composition of k rotations. We now prove that as ω_1, ω_2 approach 0, the center c approaches the point $p = (\omega_1 p_1 + \omega_2 p_2) / (\omega_1 + \omega_2)$ on the $p_1 p_2$ segment. Following [Nee98, p.38], we view the rotations by ω_1, ω_2 as reflections in lines separated

¹Unless $\omega_1 + \omega_2 = 2\pi$, which will never occur with small rotations.

by $\omega_1/2, \omega_2/2$. Then c is the intersection of two reflection lines, as illustrated in Fig. 8. With $p_1 = (0, 0)$ and $p_2 = (1, 0)$, explicit calculation yields

$$c = \left(\frac{\sin \omega_2}{\sin \omega_1 + \sin \omega_2}, \frac{\sin \omega_1 \sin \omega_2}{\sin \omega_1 + \sin \omega_2} \right).$$

From this expression and that for p above, further calculation shows that the error $\delta = |c - p|$ is $\frac{1}{8}(\omega_1 + \omega_2)$ for small ω_i . So indeed δ approaches zero.

Repeating the argument for k rotations yields (via a calculation not shown here) that the error δ is bounded by $\frac{1}{2} \sum_i \ell_i \omega_i$, where $\ell_i = |p_{i+1} - p_i|$ are the link lengths of the chain, as $\omega_i \rightarrow 0$. Thus, $\delta \rightarrow 0$, c approaches p , and the claim of the lemma is established. \square

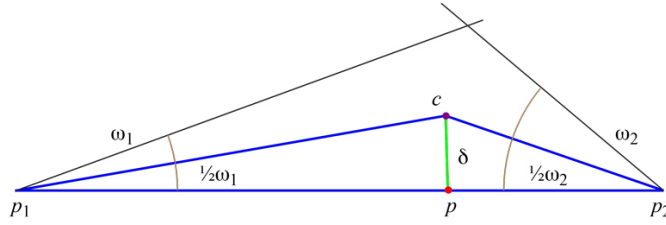


Figure 8: The error δ between the true composite center c and the center-of-gravity center.

An immediate implication of Lemma 1 is:

Lemma 2 *Under the same assumptions, the center-of-gravity approximate center p approaches a point in the convex hull of $\{p_1, \dots, p_k\}$ as $\varepsilon \rightarrow 0$, or equivalently, as $\omega \rightarrow 0$.*

Proof: With $\omega_i \geq 0$, the weighted sum in Lemma 1 is a convex combination of the p_i points, and so inside (or on the boundary of) the convex hull. \square

References

- [LO17] Anna Lubiw and Joseph O'Rourke. Angle-monotone paths in non-obtuse triangulations. In *Proc. 29th Canad. Conf. Comput. Geom.*, August 2017. arXiv:1707.00219 [cs.CG]; <https://arxiv.org/abs/1707.00219>.
- [Nee98] Tristan Needham. *Visual Complex Analysis*. Oxford University Press, 1998.
- [O'R17] Joseph O'Rourke. Edge-unfolding nearly flat convex caps. arXiv:1707.01006v2 [cs.CG]. <http://arxiv.org/abs/1707.01006>, 2017.